The Plant Cell, Vol. 17, 3378–3389, December 2005, www.plantcell.org © 2005 American Society of Plant Biologists

An *Arabidopsis* Endo-1,4-β-D-Glucanase Involved in Cellulose Synthesis Undergoes Regulated Intracellular Cycling [W]

Stéphanie Robert,[a] Adeline Bichet,[a,1] Olivier Grandjean,[b] Daniel Kierzkowski,[a,2] Béatrice Satiat-Jeunemaître,[c] Sandra Pelletier,[a] Marie-Theres Hauser,[d] Herman Höfte,[a] and Samantha Vernhettes[a,3]

[a] Laboratoire de Biologie Cellulaire, Institut Jean-Pierre Bourgin, Institut National de la Recherche Agronomique, 78026 Versailles Cedex, France

[b] Laboratoire Commun de Cytologie, Institut Jean-Pierre Bourgin, Institut National de la Recherche Agronomique, 78026 Versailles Cedex, France

[c] Dynamique de la Compartimentation Cellulaire, Institut des Sciences du Végétal, Centre National de la Recherche Scientifique Unité Propre de Recherche 2355, 91198 Gif sur Yvette Cedex, France

[d] Institute of Applied Genetics and Cell Biology, BOKU, University of Natural Resources and Applied Life Science, A-1190 Vienna, Austria

The synthesis of cellulose microfibrils requires the presence of a membrane-bound endo-1,4-β-D-glucanase, KORRIGAN1 (KOR1). Although the exact biochemical role of KOR1 in cellulose synthesis is unknown, we used the protein as a marker to explore the potential involvement of subcellular transport processes in cellulose synthesis. Using immunofluorescence and a green fluorescent protein (GFP)–KOR1 fusion that complemented the phenotype conferred by the *kor1-1* mutant, we investigated the distribution of KOR1 in epidermal cells in the root meristem. KOR1 was localized in intracellular compartments corresponding to a heterogeneous population of organelles, which comprised the Golgi apparatus, FM4-64–labeled compartments referred to as early endosomes, and, in the case of GFP-KOR1, the tonoplast. Inhibition of cellulose synthesis by isoxaben promoted a net redistribution of GFP-KOR1 toward a homogeneous population of compartments, distinct from early endosomes, which were concentrated close to the plasma membrane facing the root surface. A redistribution of GFP-KOR1 away from early endosomes was also observed in the same cells at later stages of cell elongation. A subpopulation of GFP-KOR1–containing compartments followed trajectories along the plasma membrane, and this motility required intact microtubules. These observations demonstrate that the deposition of cellulose, like chitin synthesis in yeast, involves the regulated intracellular cycling of at least one enzyme required for its synthesis.

INTRODUCTION

Cellulose, the most abundant biopolymer on earth, shows a unique structure with remarkable mechanical properties. It consists of crystalline assemblies of parallel 1,4-β–linked glucan chains, which show a tensile strength comparable to that of steel. The synthesis and assembly of those microfibrils require a specialized cellular machinery, which in land plants and Charophycean algae corresponds to plasma membrane–embedded hexameric protein complexes or rosettes (for a recent review, see Doblin et al., 2002). The deposition of microfibrils is oriented and thus controls the mechanical properties of the cell wall, which in turn determines the growth direction and the final shape of plant cells and organs. The synthesis and deposition of cellulose are highly regulated in expanding cells and during the deposition of the secondary cell wall. Very little is known about the molecular mechanisms of this regulation in plants, but it involves both transcriptional and posttranscriptional processes. The cellulose synthase complex contains multiple cellulose synthase catalytic (CESA) subunits. The *Arabidopsis thaliana* genome encodes 10 CESA isoforms, 6 of which are conserved among monocots and dicots (Doblin et al., 2002). Genetic evidence shows that at least three isoforms are involved in the synthesis of primary walls in growing cells (Fagard et al., 2000; Scheible et al., 2001; Desprez et al., 2002; Ellis et al., 2002) and three other isoforms are involved in the deposition of secondary walls in xylem cells (Taylor et al., 1999, 2000, 2003). Immunoprecipitation experiments with the secondary wall–specific isoforms suggest that they physically interact and are part of the same complex (Taylor et al., 2003). Similar observations have been made for the isoforms specific to primary walls (M. Gonneau, unpublished data). Studies in cotton (*Gossypium hirsutum*) fiber extracts identified sitosterol glucoside as a primer for the synthesis of cellulose (Peng et al., 2002), although a generalization of these findings to other systems remains controversial (for discussion, see Schrick et al., 2004). The endo-1,4-β-D-glucanase KORRIGAN1 (KOR1) is another essential enzyme for cellulose synthesis, as shown by the severely cellulose-deficient phenotype

[1] Current address: Atragene Bioinformatics, 10 Allée des Champs Elysées, 91042 Evry Cedex, France.

[2] Current address: Laboratory of General Botany, Faculty of Biology, Adam Mickiewicz University, Umultowsa 89, 61-614 Poznan, Poland.

[3] To whom correspondence should be addressed. E-mail samantha.vernhettes@versailles.inra.fr; fax 33130833099.

The author responsible for distribution of materials integral to the findings presented in this article in accordance with the policy described in the Instructions for Authors (www.plantcell.org) is: Samantha Vernhettes (samantha.vernhettes@versailles.inra.fr).

[W] Online version contains Web-only data.

Article, publication date, and citation information can be found at www.plantcell.org/cgi/doi/10.1105/tpc.105.036228.

of loss-of-function mutants in the corresponding gene (for review, see Molhöj et al., 2002). The enzyme produced in *Pichia pastoris* cleaves nonsubstituted but noncrystalline 1,4-β–linked glucan chains and shows no activity against xyloglucans (Molhöj et al., 2001; Master et al., 2004). Despite the fact that an endo-1,4-β-D-glucanase is also required for cellulose synthesis in bacteria (Molhoj et al., 2002), the exact function of KOR1 during cellulose synthesis is not clear. It has been proposed, although without convincing evidence, that KOR1 is involved in recycling sterol glucoside primers (Robert et al., 2004). On the other hand, KOR1 might remove noncrystalline glucan chains and/or relieve tensional stress, which presumably is generated during the assembly of the large number of glucan chains into a microfibril. In contrast with other endo-1,4-β-D-glucanases, KOR1 is an integral type II membrane protein. Sucrose density gradients on microsomes from tomato (*Lycopersicon esculentum*) seedlings and free-flow electrophoresis on membranes from *Arabidopsis* cell suspension cultures localized KOR1 at least partially to the plasma membrane but also to intracellular fractions (Brummell et al., 1997; Nicol et al., 1998). Zuo et al. (2000) expressed a KOR1–green fluorescent protein (GFP) fusion protein in tobacco (*Nicotiana tabacum*) BY2 cells and observed the accumulation of the fusion protein in the nascent cell plate and in punctate intracellular structures.

In this study, we observed by confocal laser scanning microscopy the subcellular localization of KOR1 in expanding root epidermal cells using specific antibodies and a GFP fusion protein. KOR1 was detected exclusively in a heterogeneous population of intracellular compartments. These compartments comprised both the Golgi apparatus and the FM4-64–labeled compartments referred to as early endosomes. At least a subpopulation of these compartments displayed trajectories along the plasma membrane, and this motility required intact microtubules. Interestingly, the inhibition of cellulose synthesis with isoxaben led to a rapid redistribution of GFP-KOR1 to a homogeneous population of compartments distinct from endosomes, adjacent to the plasma membrane facing the root surface. Redistribution away from the early endosomes was also observed in the same cells at later stages of cell elongation, during which more cellulose was produced than at earlier growth stages. These data demonstrate that cellulose deposition involves the regulated intracellular cycling of at least one enzyme involved in its synthesis.

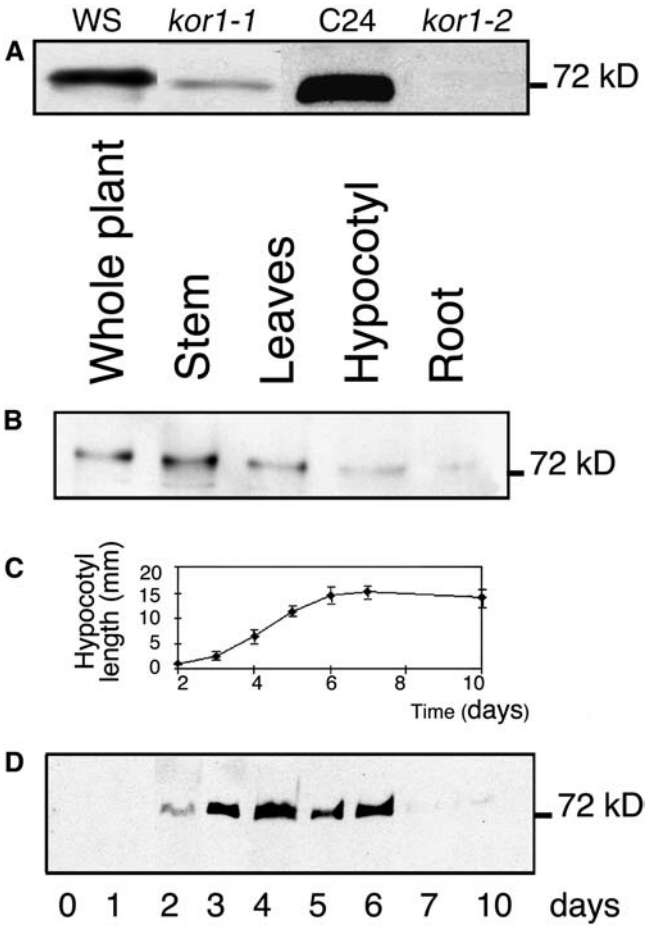

Figure 1. KOR1 Is Ubiquitously Expressed and Its Level Correlates with Cell Elongation in Dark-Grown Hypocotyls.

(A) Specificity of αNKOR1. Crude extracts were prepared from 5-d-old seedlings grown in light conditions (*kor1-1* and *kor1-2* were in the Wassilewskija [Ws] and C24 background, respectively).
(B) Left to right, crude extracts of entire wild-type plants and from stem, leaves grown for 28 d in greenhouse, and hypocotyls and roots of 7-d-old wild-type plants grown in light conditions.
(C) Time course of hypocotyl growth of dark-grown seedlings.
(D) Left to right, crude extracts of seeds and in vitro dark-grown seedlings (2 to 10 d). Error bars represent SE.
In **(A)**, **(B)**, and **(D)**, immunoblots were probed with αNKOR1. Ten micrograms of total protein was loaded in each lane.

RESULTS

Expression Pattern of KOR1

An affinity-purified polyclonal antiserum against the N-terminal cytosolic domain of KOR1, referred to as αNKOR1, recognized a unique 72-kD band on immunoblots of crude extracts prepared from wild-type *Arabidopsis* seedlings. Extracts from seedlings homozygous for the leaky *kor1-1* allele and the null *kor1-2* allele showed a weak band and no band at all, respectively, demonstrating the specificity of the antiserum (Figure 1A). This antiserum recognized a protein in all growing plant organs, such as stems, leaves, roots, and hypocotyls (Figure 1B). KOR1 was undetectable in imbibed seeds and appeared during germination in dark-grown seedlings, peaked during the growth phase of the hypocotyl, and disappeared again at the end of the elongation phase (Figures 1C and 1D). In light-grown conditions, a similar pattern was observed except that KOR1 expression remained detectable also after hypocotyl growth arrest (data not shown).

KOR1 Accumulates in Intracellular Compartments

To study the subcellular localization of KOR1, we performed immunolocalization with αNKOR1 in root cells. Surprisingly, no

KOR1 labeling was detected in the plasma membrane (Figure 2) or in the developing cell plate in dividing cells (data not shown). By contrast, the antibody revealed an intracellular punctate staining pattern in *Arabidopsis* root cells (Figures 2A and 2B). No KOR1 labeling was detected in the null allele *kor1-2* (Figure 2C), confirming again the specificity of the antibody. As an additional control, root cells of wild-type plants expressing a c-myc–tagged version of KOR1 from the cauliflower mosaic virus *35S* promoter were doubly labeled with αNKOR1 (Figure 2D) and a monoclonal anti-c-myc antibody (Figure 2E). The c-myc–tagged protein was still functional in that it was able to complement the hypocotyl and root phenotype of the *kor1-1* mutant (data not shown). Both antibodies colocalized, again confirming the specificity of the immunolabeling (Figure 2F).

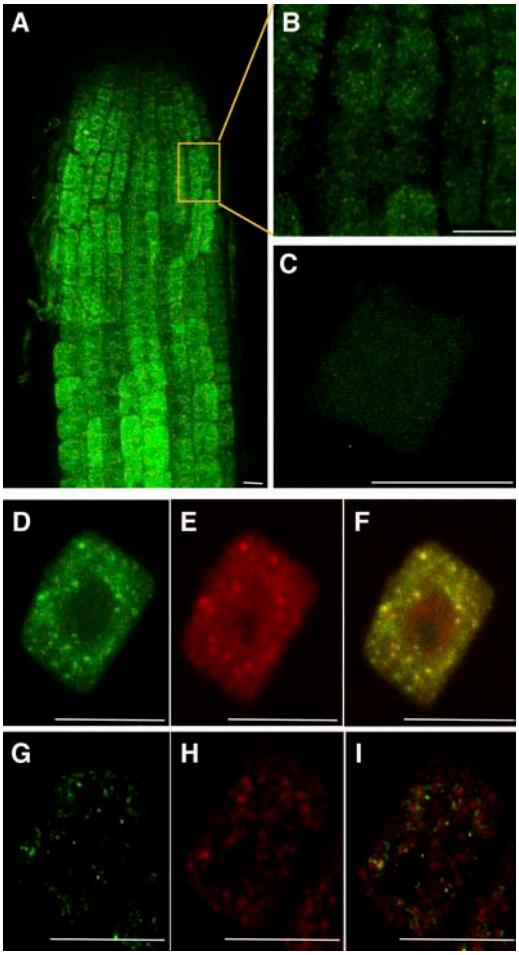

Figure 2. KOR1 Is Present in Intracellular Organelles, a Subpopulation of Which Corresponds to the Golgi Apparatus.

Confocal images of immunofluorescence staining with αNKOR1 (**[A]** to **[D]** and **[G]**) and anti-c-myc antibodies (**[E]** and **[H]**) in *Arabidopsis* root cells are shown. Bars = 10 μm.

(A) and **(B)** Image projection of a wild-type root **(A)** and enlargement of an epidermal cell at the beginning of the elongation zone **(B)**. Note the presence of intracellular patches and the absence of labeling of the plasma membrane.

(C) In *kor1-2* root cells, note the absence of labeling.

(D) to **(F)** Combined image **(F)** of KOR1 **(D)** and KOR1–c-myc **(E)** in a root cell obtained from KOR1–c-myc seedlings. Both antibodies labeled the same intracellular compartment.

(G) to **(I)** Combined image **(I)** of KOR1 **(G)** and a Golgi apparatus marker, Glt6–c-myc **(H)**, in a root cell obtained from Glt6–c-myc seedlings. Note a partial colocalization of KOR1 and Glt6–c-myc.

To confirm the intracellular localization, a translational GFP-KOR1 fusion protein was expressed under the constitutive cauliflower mosaic virus *35S* promoter in homozygous *kor1-1*. To ascertain the biological activity of this construct, we compared the hypocotyl length of dark-grown seedlings and the root length of light-grown seedlings of the wild type, *kor1-1*, and the transformants (Figure 3). Although *kor1-1* seedlings exhibited their characteristic short-hypocotyl phenotype, several independent transformants developed hypocotyl length similar to that of the wild-type control (Figures 3A and 3B). The same GFP-KOR1–expressing lines showed a root length that was intermediate between *kor1-1* and wild-type roots when grown in the light (Figure 3C). It is conceivable that the partial complementation of the root phenotype is the result of a negative effect of the overexpression of the fusion protein on root growth, because the same construct also interfered slightly with root growth when expressed in a wild-type background (data not shown). In conclusion, depending on the cellular context, the GFP-KOR1 fusion protein complemented totally or partially the growth defect of *kor1-1*. The fusion protein, therefore, is at least in part targeted to the same subcellular compartments as the wild-type protein.

We next investigated the subcellular localization of the GFP-KOR1 fusion protein using confocal laser scanning microscopy on root epidermal cells in their early elongation phase (cell length between 8 and 30 μm). Similar to the antibody staining, a punctate GFP signal was observed (Figures 4A [corresponding to a still image of Supplemental Video 1 online] and 4C). The orthogonal projection obtained from 12 successive confocal sections showed that the GFP-KOR1–containing compartments were concentrated close to the plasma membrane (see Supplemental Video 1 online). Moreover, the tonoplast was strongly labeled, which was not observed with αNKOR1 in wild-type plants or in plants overexpressing the KOR1–c-myc construct from the same *35S* promoter. Therefore, the tonoplast labeling must be related to the properties of the GFP fusion protein. Again, no labeling of the plasma membrane was observed, and despite numerous attempts, we have never observed cell plate labeling in dividing root cells, embryonic cells, or *Arabidopsis* cell suspension cultures (data not shown).

KOR1-Containing Compartments Are Heterogeneous and Comprise Both the Golgi Apparatus and Early Endosomes

To characterize the intracellular compartments, we first performed double-labeling experiments with αNKOR1 and anti-c-myc on roots expressing the Golgi-localized protein Glt6–c-myc (Figures 2G to 2I) (Dunkley et al., 2004). KOR1 partially colocalized with the Golgi marker. The intracellular distribution of KOR1 varied in different cell types and plant species. For instance, no colocalization was observed in maize (*Zea mays*) root cells labeled with αNKOR1 and JIM84, an antibody raised against a glycan epitope present in the Golgi apparatus and plasma

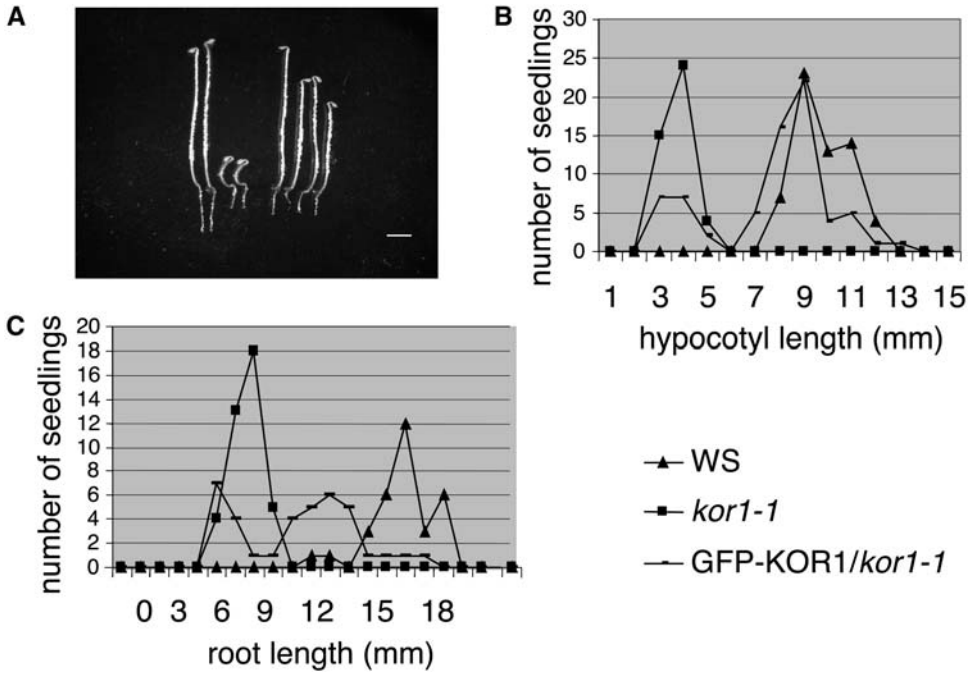

Figure 3. The Overexpression of GFP-KOR1 in *kor1-1* Totally Restores Hypocotyl Growth and Partially Restores Root Growth.

(A) Four-day-old dark-grown seedlings of Ws (left, two seedlings), *kor1-1* (middle, two seedlings), and GFP-KOR1/*kor1-1* (right, two seedlings). Bar = 1 mm.

(B) Distribution of hypocotyl length of 4-d-old dark-grown Ws, *kor1-1*, and GFP-KOR1/*kor1-1* seedlings.

(C) Distribution of root length of 4-d-old light-grown Ws, *kor1-1*, and GFP-KOR1/*kor1-1* seedlings.

membrane (data not shown). Together, these observations indicate that KOR1 accumulated in a heterogeneous population of compartments, which can comprise the Golgi apparatus depending on the cellular context.

To further characterize the heterogeneous population of KOR1-containing compartments, we used the fluorescent styryl dye FM4-64, which is known to follow the endocytic pathway, from the plasma membrane via endosomes to the vacuole, when exogenously added to yeast (Vida and Emr, 1995) or plant cells (Ueda et al., 2001). Immediately after adding FM4-64, the plasma membrane of root epidermal cells was labeled. Ten minutes later, FM4-64 appeared in intracellular compartments, which, given the short internalization times, are thought to correspond to early endosomes (Grebe et al., 2003; Bolte et al., 2004). These compartments partially colocalized with GFP-KOR1, suggesting that the GFP-KOR1 in these compartments also was internalized from the plasma membrane (Figure 4F). In addition, we observed characteristic composite structures consisting of two adjacent compartments labeled, respectively, by GFP-KOR1 and FM4-64. To confirm the localization in the early endosomes, we studied the effect of the vesicle-trafficking inhibitor brefeldin A (BFA) on the dynamics of GFP-KOR1 compartments. Short-term treatments with BFA induce in root cells the reversible formation of large aggregates (Satiat-Jeunemaitre and Hawes, 1994), which contain both exocytic and endocytic material (Geldner et al., 2001; Grebe et al., 2003; Hawes and Satiat-Jeunemaitre, 2005). Roots were treated for a short time with BFA, and the localization of GFP-KOR1 was followed in root cells at different growth stages. We first observed that the responses to BFA treatments were variable among individual roots and even within the same root among cells at different growth stages. Similar observations have been reported recently and may reflect local differences in auxin concentration (Paciorek et al., 2005). In elongating cells, a 30-min BFA treatment led to the disappearance of the GFP-KOR1–labeled punctate structures and a concomitant emergence of a single large aggregate per cell (Figure 5B), without affecting the labeling of the tonoplast. This treatment was completely reversible upon withdrawal of BFA (Figure 5C). BFA-induced compartments were also observed (Figure 5F) in wild-type root cells upon immunofluorescence staining with αNKOR1. To confirm the presence of KOR1 in endosomal compartments, double labeling of KOR1 and GNOM was performed in GNOM–c-myc seedlings after BFA treatment (Figures 5F to 5H). GNOM is an ARF-GEF that mediates the endosomal recycling of PIN1, a transport facilitator of the plant hormone auxin (Geldner et al., 2003). Upon BFA treatment, we observed a partial colocalization of GNOM–c-myc and KOR1, suggesting that these proteins are present in overlapping endosomal compartments.

Together, these observations demonstrate the presence of GFP-KOR1, like endogenous KOR1, in early endosomal compartments. Actin is known to play a major role in organelle motility and vesicle trafficking (Geldner et al., 2001; Grebe et al., 2003; Hawes and Satiat-Jeunemaitre, 2005). To determine the role of actin on the localization of GFP-KOR1–labeled compartments, we treated roots with cytochalasin D (cytD), which depolymerizes actin filaments. Short treatments with cytD alone did not lead

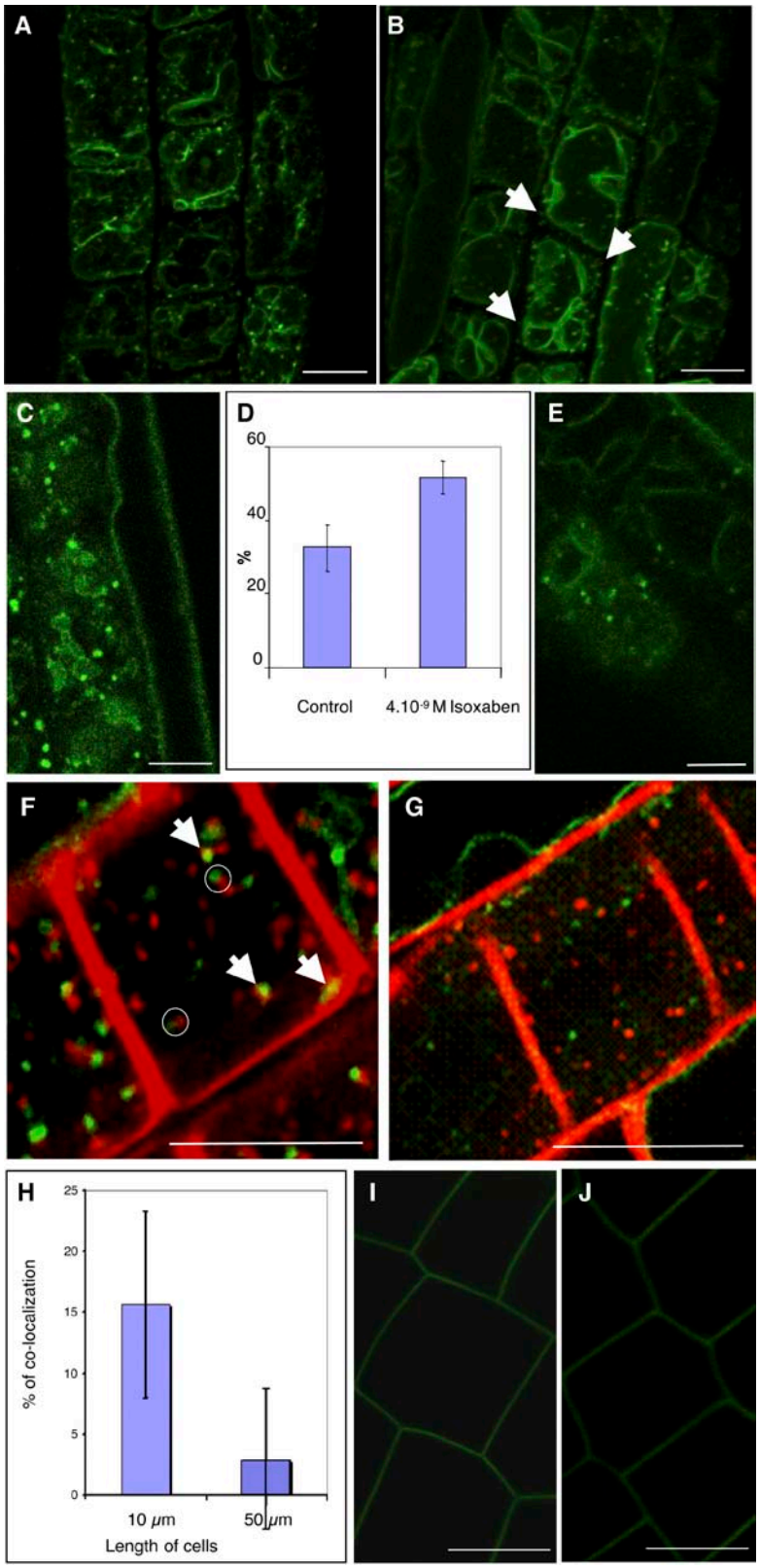

Figure 4. GFP-KOR1–Labeled Structures Lie on the Endocytic Pathway in *Arabidopsis* Root Cells, and Their Distribution Is Regulated during Isoxaben Treatment and Normal Cellular Development.

to observable changes in the distribution of the GFP-KOR1 compartments (Figure 5D). Pretreatment of cytD, however, inhibited the formation of the large BFA-induced compartment (Figure 5E). These observations confirm that the formation of the GFP-KOR1–containing BFA-induced compartment depended on an intact actin cytoskeleton.

Inhibition of Cellulose Synthesis by Isoxaben Is Accompanied by an Intracellular Redistribution of GFP-KOR1

The observations described above showed that KOR1 accumulated in a heterogeneous population of intracellular compartments. These compartments may either reflect an intracellular activity for KOR1 or may be part of a general trafficking pathway that controls the access of KOR1 to its extracellular substrate. To investigate the relation between KOR1 localization and cellulose synthesis, we first studied the localization of GFP-KOR1 in protoplasts generated from leaf mesophyll cells. Despite the highly active cellulose synthesis machinery in regenerating protoplasts, GFP-KOR1 was still present in intracellular compartments without detectable staining of the plasma membrane (data not shown).

In a second experiment, roots were treated with isoxaben, which targets the cellulose synthase catalytic subunits CESA3 and CESA6 (Scheible et al., 2001; Desprez et al., 2002) and specifically inhibits cellulose synthesis in <1 h (G. Mouille, unpublished data). Seedlings were treated with isoxaben for 1 h, and the subcellular localization of GFP-KOR1 was monitored in root epidermal cells and compared with the localization of the plasma membrane marker GFP-LTI6b (Cutler et al., 2000). In the presence of isoxaben, no accumulation in the plasma membrane was observed (Figures 4B [corresponding to a still image of Supplemental Video 2 online] and 4E). Interestingly, however, the average size and intracellular distribution of GFP-KOR1–containing compartments had changed (Figures 4B, 4D, and 4E), in contrast with the plasma membrane marker GFP-LTI6b, the localization of which was unaffected by the treatment (Figures 4I and 4J). To quantify these changes, we measured the relative surface area of the GFP-KOR1–labeled compartments and determined their intracellular distribution by counting the compartments present in successive optical sections between the external cell surface and the tonoplast and comparing this number with the total number of compartments in each cell (Figure 4D). In control cells, a broad size distribution was observed, with a median surface area of 0.42 $\pm$ 0.28 μm^2 ($n = 1133$). In isoxaben-treated cells, GFP-KOR1–labeled compartments were smaller (0.22 μm^2), more homogeneous, as shown by the narrower size distribution ($\pm$0.12 μm^2; $n = 514$), and closer to the external surface of the cells (50% of the compartments were present near the external surface of the cell compared with only 30% in the control roots [Figure 4D; see Supplemental Video 2 online]). Labeling with FM4-64 for 10 min revealed endosomal compartments in both control and isoxaben-treated seedlings (Figures 4F and 4G), indicating that, in contrast with auxin (Paciorek et al., 2005), isoxaben did not affect endocytosis per se. Interestingly, only in control cells did GFP-KOR1 partially colocalize with FM4-64 compartments, whereas in isoxaben-treated cells, no such colocalization was observed. In addition, in isoxaben-treated cells, we never observed the composite structures consisting of two adjacent compartments labeled by GFP-KOR1 and FM4-64, respectively. These results indicate that the inhibition of cellulose synthesis by isoxaben coincided with a redistribution of GFP-KOR1 out of FM4-64–labeled compartments and into a homogeneous population of smaller, polarly distributed compartments, which were detected primarily adjacent to the plasma membrane facing the root surface.

GFP-KOR1 Cycling Is Developmentally Regulated

The observations described above show that GFP-KOR1 cycles through different intracellular compartments and that the cycling dynamics can be influenced by isoxaben. We next investigated whether the cycling is regulated during different growth stages of the cell. To this end, we incubated 3-d-old roots for 10 min with FM4-64 and compared the colocalization of GFP-KOR1 with the dye in two distinct populations of epidermal cells: small cells of

Figure 4. (continued).

(A) and **(B)** Orthogonal projections from living root cells expressing GFP-KOR1 untreated **(A)** or treated with 4×10^{-9} M isoxaben for 1 h **(B)**. Isoxaben treatment induces a redistribution of GFP-KOR1 compartments. Arrows indicate the dots at the tops of the cells. The strong background labeling corresponds to the tonoplast.

(C) and **(E)** Single optical sections of a root epidermal cell expressing GFP-KOR1 untreated **(C)** or treated with 4×10^{-9} M isoxaben for 1 h **(E)**. Note the heterogeneous population of KOR1-labeled structures localized close to the cell surface in untreated root cells. A more homogeneous population of smaller compartments is detected in isoxaben-treated cells.

(D) Percentage of dots present at the tops of cells expressing GFP-KOR1 treated with or without 4×10^{-9} M isoxaben for 1 h. Note the redistribution of GFP-KOR1 toward the cortical region of cells upon isoxaben treatment. Error bars represent SE.

(F) and **(G)** Single optical sections of a cell colabeled with FM4-64 and GFP-KOR1 in root cells untreated **(F)** or treated with 4×10^{-9} M isoxaben for 1 h **(G)**. Note that some GFP-KOR1 colocalized with FM4-64 after 10 min of incubation (arrows) in untreated root cells. When not colocalized, they frequently appeared adjacent to each other (open circles). Note that upon isoxaben treatment, no colocalization was observed between GFP-KOR1 compartments and FM4-64–labeled structures, suggesting that isoxaben caused the redistribution of GFP-KOR1 away from early endosomes.

(H) Percentage of colocalization of FM4-64–labeled structures and GFP-KOR1 compartments in root cells from different growth stages. In smaller cells (10 μm), 15% of the GFP-KOR1 compartments colocalized with the early endosomal marker, compared with only 2.5% in the larger cells (cells between 50 and 70 μm). Error bars represent SE.

(I) and **(J)** Single optical sections of a cell expressing the plasma membrane GFP-LTI6b fusion protein untreated **(I)** or treated with 4×10^{-9} M isoxaben for 1 h **(J)**. No intracellular labeling was observed upon isoxaben treatments.

Bars = 10 μm.

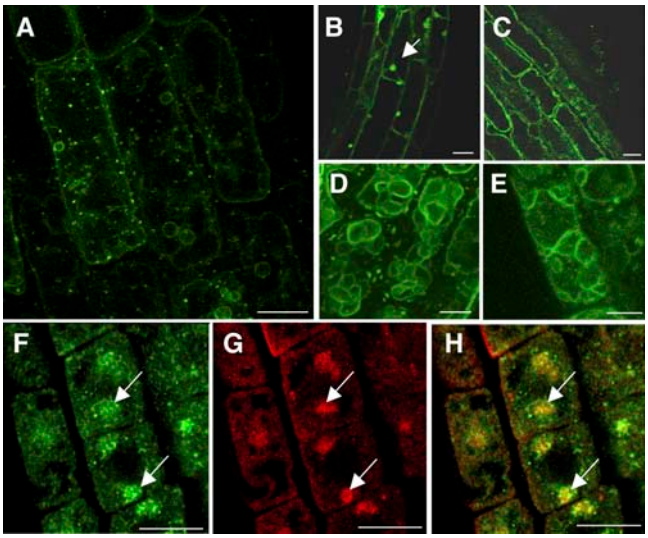

Figure 5. Reversible Inhibition of Actin-Dependent GFP-KOR1 Recycling by BFA Treatment.

(A) to **(E)** Single optical sections of elongating root cells treated with buffer control for 30 min **(A)** or with 50 μM BFA for 30 min **(B)**, pretreated with 20 μM cytD for 15 min followed by 50 μM BFA and 20 μM cytD for 45 min **(C)**, treated with 20 μM cytD for 45 min **(D)**, or treated with 50 μM BFA for 30 min followed by a 90-min washout of BFA **(E)**. Note the presence of BFA compartment(s) in elongating cells (see arrow) **(B)** and their absence in the presence of cytD **(C)**.

(F) to **(H)** Colocalization **(H)** of KOR1 **(F)** and GNOM **(G)** by immunofluorescence staining of root epidermal cells of seedlings expressing GNOM–c-myc. αNKOR1 **(F)** and c-myc **(G)** antibodies show that KOR1 and GNOM are present in the same BFA-induced compartments (see arrows). Bars = 10 μm.

10 μm in their early elongation phase, and larger but still rapidly expanding cells more proximally in the root elongation zone (50 to 70 μm). Fourier transform infrared microspectroscopy showed that the relative cellulose content was higher in the larger cells than in the smaller cells (G. Mouille, personal communication). Individual cells in both cell populations showed large variations in colocalization, which may reflect local variations in auxin, as described by Paciorek et al. (2005), or some other critical factor(s). Interestingly, despite these large variations, highly significant differences were observed in the colocalization between the two cell populations (Figure 4H). Indeed, in smaller cells, on average 15% of the GFP-KOR1 compartments colocalized with the early endosomal marker, compared with only 2.5% in the larger cells. These results demonstrate that the intracellular cycling of GFP-KOR1 was developmentally regulated, with a preferential mobilization out of FM4-64–labeled compartments in larger cells with higher relative cellulose contents.

The Motility of GFP-KOR1 Compartments Requires Intact Microtubules

To study the motility of GFP-KOR1 compartments, we produced time-lapse videos of root cells. The video (Figure 6G corresponds to a still image of Supplemental Video 3 online) shows that at least a subpopulation of these compartments was motile and showed linear trajectories parallel to the plasma membrane. Cortical microtubules, like cellulose microfibrils, form transversely oriented arrays in elongating cells. Evidence that microtubules can orient the deposition of microfibrils exists, but the exact mechanistic link between microtubule orientation and cellulose deposition is not understood (Baskin, 2001; Wasteneys, 2004). Given the key role for KOR1 in cellulose synthesis, it is conceivable that the movement of the GFP-KOR1 compartments is related to the oriented deposition of the cellulose microfibrils. Therefore, we investigated whether there was a link between the directional movements of the GFP-KOR1 compartments and microtubules. Seedlings were treated for 10 min with 10 μM oryzalin to depolymerize microtubules (Figures 6B and 6E). Interestingly, this treatment completely abolished the motility of GFP-KOR1–labeled compartments (data not shown), which indicated that the dynamic behavior of GFP-KOR1 compartments, in contrast with early endosomes or the Golgi apparatus (Grebe et al., 2003), depended on the presence of intact microtubules. The oryzalin treatment also caused the formation of GFP-KOR–containing aggregates (Figures 6A and 6D). As a control, similar oryzalin treatments did not provoke clusters of the plasma membrane GFP-LTI6b fusion protein (Figures 6C and 6F) or of a Golgi marker (Satiat-Jeunemaitre and Hawes, 1992; G. Mouille, personal communication), indicating that oryzalin specifically disturbed the localization of GFP-KOR1 compartments.

Using manual tracking (Figure 6G), the average velocity of these compartments was evaluated at 1.7 ± 0.31 μm/min, whereas acceleration and deceleration phases could be observed with peak velocities of up to 5.8 μm/min. The average velocity is much lower than that reported for the Golgi apparatus (4.2 μm/s) (Nebenfuhr et al., 1999) and processive myosin movement on actin (7 μm/s) (Tominaga et al., 2003) and is closer to the velocity of kinesin movement on microtubules (Marcus et al., 2002; Ambrose et al., 2005).

DISCUSSION

KOR1 Endo-1,4-β-D-Glucanase Cycles through Subcellular Compartments

Although the exact role of the endo-1,4-β-D-glucanase KOR1 in the synthesis of cellulose remains to be determined, this enzyme is an essential component of the cellulose synthesis machinery (Nicol et al., 1998; His et al., 2001; Lane et al., 2001; Sato et al., 2001; Szyjanowicz et al., 2004). In addition, the substrate of this enzyme produced in a heterologous system is cellulose and not xyloglucan (Molhoj et al., 2001; Master et al., 2004). Such an enzyme would be expected to be present in the plasma membrane in the presence of its substrate. Our results, however, show that KOR1 accumulates in intracellular compartments. First, antibodies raised against the intracellular or the extracellular domain (data not shown) of KOR1 labeled intracellular organelles and not the plasma membrane. Second, the same localization was detected in plants expressing a functional P_{35S}-KOR1–c-myc fusion protein using immunodetection with anti-c-myc and αNKOR1 antibodies. Third, a constitutively expressed GFP-KOR1 fusion

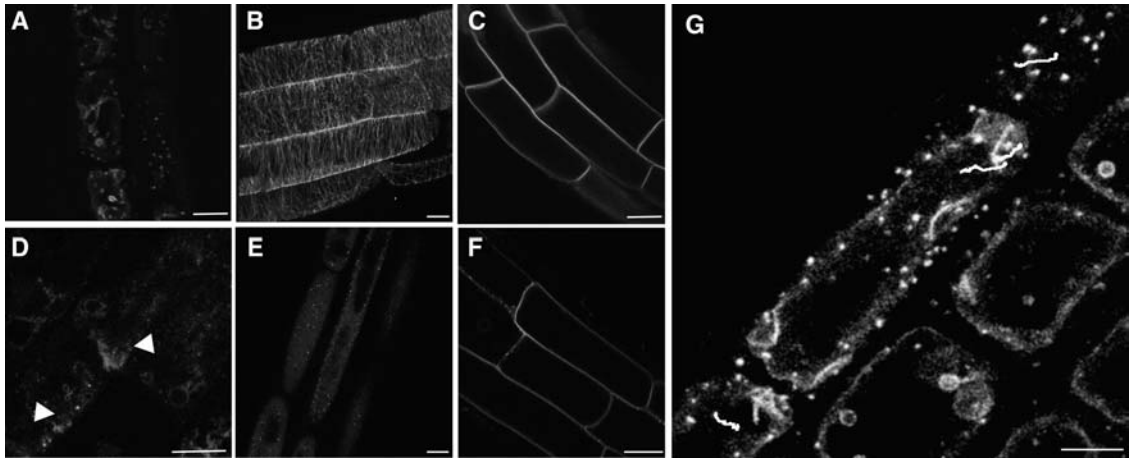

Figure 6. GFP-KOR1 Localization Is Affected by the Microtubule-Depolymerizing Drug Oryzalin.

(A) to **(F)** Single optical sections of root cells expressing GFP-KOR1 (**[A]** and **[D]**), MAP4-GFP, which labels microtubules (**[B]** and **[E]**), or GFP-LTI6b, a plasma membrane protein (**[C]** and **[F]**) untreated (**[A]** to **[C]**) or after treatment with 10 μM oryzalin for 10 min (**[D]** to **[F]**). Note the localization of GFP-KOR1 compartments in aggregates after oryzalin treatment (arrowheads).

(G) Manual tracking of four linear trajectories of GFP-KOR1–containing compartments for 4 min illustrated by white lines.

Bars = 10 μm.

protein was also observed in similar intracellular compartments and not in the plasma membrane. Although Zuo et al. (2000) observed the accumulation of a KOR1-GFP fusion protein in the cell plate of dividing tobacco BY2 cells, we never detected cell plate labeling in dividing cells with the anti-KOR1 antibodies or the GFP-KOR1 fusion protein. This discrepancy may be attributable to differences of the cellular systems (BY2 versus *Arabidopsis* root or embryonic cells) or to differences in the properties of the respective fusion proteins. Indeed, Zuo et al. (2000) used a C-terminal GFP fusion to KOR1, deleting the three terminal amino acids. To our knowledge, this fusion protein has not been tested for its complementation of the phenotype conferred by the *kor1* mutant.

The intracellular KOR1-containing compartments comprised both the Golgi apparatus and early endosomes, as shown by their colocalization with the Golgi marker Glt6–c-myc and FM4-64, respectively. In <30 min of BFA treatment, large GFP-KOR1–labeled compartments were observed, the formation of which was reversible and actin-dependent. It was shown recently that the intracellular distribution of polarly localized putative transport facilitators for the plant hormone auxin, PIN1 and PIN2, is also sensitive to BFA (Geldner et al., 2001; Grebe et al., 2003). PIN1 and PIN2 recycle between the plasma membrane and endosomes, and in the case of PIN1, the BFA-sensitive guanine exchange factor of ARF-type G proteins, GNOM, mediates this cycling (Geldner et al., 2003). GNOM-GFP also partially colocalizes with FM4-64–labeled early endosomes upon its internalization. In plants harboring a variant version of GNOM mutated in the sec7 domain, PIN1 trafficking was fully insensitive to BFA, whereas the sensitivity of PIN2 transport was weakly affected, suggesting that different BFA-sensitive ARF-GEFs contribute to the endocytic pathway. Upon BFA treatment of GNOM–c-myc seedlings, KOR1 and GNOM colocalized in the same compartments, suggesting that KOR1 also undergoes endocytosis from the plasma membrane. It will be interesting to determine whether GNOM also controls the endosomal trafficking of KOR1.

In apparent contrast with the in situ immunolabeling results, immunoblotting revealed KOR1 in fractions enriched for plasma membrane markers obtained by sucrose density gradients (Brummell et al., 1997), free-flow electrophoresis (Nicol et al., 1998), or two-phase partitioning (S. Vernhettes, unpublished data). Because no endosomal markers were used in these experiments, it cannot be excluded that these plasma membrane–enriched fractions contained membranes of endosomal origin. Alternatively, the absence of plasma membrane labeling with in situ localization techniques may simply reflect the higher concentration of KOR1 in intracellular compartments and the dilution of the protein in the plasma membrane. Together, our results suggest that KOR1 cycles through different intracellular compartments and presumably through the plasma membrane.

Cycling between the plasma membrane and early endosomes was also observed in animal cells for the glucose transporter GLUT4 (for a recent review, see Bryant et al., 2002) and the AMPA receptor (Mikyoung et al., 2004) and in yeast for chitin synthase Chs3p (Valdivia and Schekman, 2003) and the amino acid permease GAP1 (Roberg et al., 1997). The complex distribution of the protein in the plasma membrane, sorting endosomes, recycling endosomes, the *trans*-Golgi network, and transport vesicles reflects an equilibrium within a dynamic transport itinerary. For example, insulin acts upon this balance in adipocytes and as a result causes a rapid mobilization of the GLUT4 transporter to the cell surface, which facilitates the rapid reduction of plasma glucose levels. Similar observations have been reported for chitin synthase Chs3p in yeast, which in normal physiological conditions accumulates in early endosomes (also referred to as chitosomes) (Valdivia and Schekman, 2003). Challenging cells with wall-damaging agents favors a shift of Chs3p from chitosomes to the plasma membrane as part of a cell wall repair

mechanism. This regulated secretion allows the fine-tuning of the activity through the mobilization of an intracellular reservoir of chitin synthase.

If the KOR1-containing compartments exhibit similar dynamics in plant cells, one might expect a change in the relative distribution of KOR1 between the intracellular compartments and the plasma membrane in response to an increased demand for cellulose synthesis. Our experiments on protoplasts or with isoxaben do not provide evidence for a dramatic change in partitioning between intracellular compartments and the cell surface. However, upon isoxaben treatment, a change occurred in the intracellular distribution of GFP-KOR1, which preferentially accumulated in a homogeneous population of smaller compartments distinct from endosomes close to the external cell surface. This suggests that isoxaben has an effect on the intracellular cycling dynamics of KOR1. What could be the relationship between the isoxaben treatment and the altered localization of KOR1? Two scenarios can be envisaged. First, KOR1 may be a cargo protein of the same vesicles as the targets of isoxaben CESA3 and CESA6. The primary action of isoxaben could be the inhibition of the trafficking of these vesicles toward the plasma membrane through interaction with CESA3 and CESA6, which also would inhibit the insertion of KOR1 into the plasma membrane. The inhibition in cellulose synthesis could be an indirect result of this trafficking block. Alternatively, isoxaben could interfere with the action of CESA3 and CESA6 through some other mechanism. Reduced cellulose synthesis in turn could lead, via a feedback mechanism, to an increased mobilization of KOR1, and maybe the entire cellulose synthase complex, away from the early endosomes into a regulated secretory compartment, out of which these proteins may be distributed to well-defined locations at the cell surface. The preferential presence of this compartment close to the external cell surface is consistent with the much higher demand for cellulose synthesis in external walls compared with internal walls.

The increased mobilization of GFP-KOR1 away from early endosomes observed at more advanced stages of epidermal cell elongation in the root suggests that the intracellular cycling of KOR1 is also highly regulated during normal cellular development. This remobilization also would be consistent with an increased demand for cellulose synthesis observed in these cells.

The Motility of the GFP-KOR1 Compartments Depends on Intact Microtubules

Time-lapse videos showed that GFP-KOR1–containing compartments were motile. The observed heterogeneity of the dynamic behavior of the compartments is in agreement with their heterogeneous nature. A subpopulation followed linear trajectories along the plasma membrane. The velocity of these compartments was lower than that of the Golgi apparatus and more in line with the movement of kinesin motors on microtubules. Oryzalin treatment abolished this motility within 10 min, indicating an essential role for microtubules in the motility of these GFP-KOR1 compartments, in contrast with the Golgi apparatus (Boevink et al., 1998) or early endosomes, the motility of which is not affected by microtubule inhibitors (Grebe et al., 2003). These observations shed an interesting new light on a long-standing controversy regarding the relationship between the orientation of cortical microtubules and the synthesis of cellulose microfibrils. In elongating cells, both cortical microtubules and the innermost microfibrils of the primary cell wall are transversely oriented to the elongation axis (Baskin, 2001; Wasteneys, 2004). Coalignment between microtubules and microfibrils also can be observed in regenerating protoplasts with taxol-stabilized microtubules (Melan, 1990). Also, in xylem elements, microtubule arrays coincide with the site of synthesis of microfibrils of the secondary cell wall thickenings (Gardiner et al., 2003). Disorganization of microtubules can also lead to a perturbed microfibril orientation, as shown in mutants for the katanin P60 subunit *bot1/fra2* (Burk and Ye, 2002). A popular model proposes that microtubules guide the movement of cellulose synthase complexes in the plasma membrane either directly via motor proteins or indirectly by constraining the path of the complexes through direct contacts with plasma membrane proteins. Recent experiments with *Arabidopsis* roots, using the cellulose synthesis inhibitor dichlorobenzonitrile an a temperature-sensitive microtubule mutant, *mor1-1* (Himmelspach et al., 2003), showed that this view most likely is an oversimplification. Indeed, the results show that perturbing microtubules by shifting the mutant to a restrictive temperature did not perturb the orientation of the most recently deposited microfibrils. Although it remains to be shown whether KOR-containing compartments interact with microtubules, our observations support an alternative hypothesis in which microtubules do not necessarily control the movement of the cellulose synthase complexes in the plasma membrane, which could be propelled by the polymerization of the β-1,4-glucan chains into a linear movement. Rather, microtubules might influence the position of KOR1-containing organelles and in this way favor the insertion of KOR1 and perhaps the entire complex to well-defined positions in the plasma membrane. In this view, the removal of microtubules would not affect the movement of already inserted complexes. A comparable hypothesis, in which microfibrils are oriented through the control of the insertion of the cellulose synthase complexes in the plasma membrane, has been proposed by Mulder et al. (2004).

It has been suggested that COB, an extracellular glycosylphosphatidylinositol–anchored protein, is required for the oriented deposition of cellulose microfibrils and is aligned in narrow bands perpendicular to the longitudinal axis in cells undergoing rapid elongation. Like for GFP-KOR1–containing compartments, COB localization also depends on the presence of cortical microtubules (Roudier et al., 2005). The relationship between COB and the localization and motility of KOR1 compartments remains to be determined.

In conclusion, this study shows that at least one enzyme is involved in the synthesis of cellulose cycles through intracellular compartments and presumably the plasma membrane. This cycling is regulated during normal cell expansion, which may play a role in the control of cellulose synthesis. The microtubule-dependent motility of GFP-KOR1–containing compartments may play a role in the delivery of KOR1 and perhaps the cellulose synthase complexes to specific locations in the plasma membrane.

While this article was in preparation, Paradez and colleagues showed that a functional yellow fluorescent protein (YFP)–CESA6 fusion protein also accumulated in a heterogeneous population

of intracellular compartments in *Arabidopsis* root and hypocotyl cells and that isoxaben treatment also caused an intracellular redistribution of YFP-CESA6. In addition, a subset of fluorescent objects displayed linear trajectories at the cell surface (A.R. Paredez, D. Ehrhardt, and C. Somerville, unpublished data). It will be interesting to investigate the relationship between the CESA6- and KOR1-containing compartments.

METHODS

Plant Strains and in Vitro Growth Conditions

Seeds of *Arabidopsis thaliana* ecotypes Ws and Columbia were provided by K. Feldman (University of Arizona, Tucson, AZ). Mutants used were *kor1-1* (Nicol et al., 1998) and *kor1-2*, which was kindly provided by N.-H. Chua (Zuo et al., 2000). The GNOM–c-myc and the GFP-LTI6b (stock center number N84726) (Cutler et al., 2000) lines were kindly provided by G. Jürgens. The Glt6–c-myc line was kindly provided by P. Dupree (Dunkley et al., 2004).

Arabidopsis seedlings were grown on solid medium as described by Estelle and Somerville (1987) without sucrose at 20°C. Seeds were cold-treated for 48 h to synchronize germination. For dark-growth conditions, seeds were exposed to fluorescent white light (200 $\mu mol \cdot m^{-2} \cdot s^{-1}$) for 4 h to induce germination, and the plates were wrapped in three layers of aluminum foil. The age of the seedlings was counted from the beginning of the light treatment.

For light-growth conditions, plants were grown in a 16-h-light/8-h-dark cycle.

Chemical Treatments

Three-day-old light-grown seedlings were treated with 4×10^{-9} M isoxaben for 1 h, 50 μM BFA for 30 min, and 10 μM oryzalin for 10 min. The initial stocks of isoxaben and BFA were in DMSO, and to obtain the appropriate concentration in the culture medium, the stocks were diluted at least 1000-fold. Cells in living roots were stained with 50 μM FM4-64 (Molecular Probes).

Construction of GFP-KOR1

The construct was made using Gateway cloning technology (Invitrogen). In short, the full-length cDNA of *KOR1* was amplified by PCR using the primer KOR1U containing the 1/2 attB1 recombination site and the start codon of the *KOR1* gene (5′-AAAAAAGCAGGCTCCATGTACGGAAGA-GATCCATGGGGAGGT-3′) and the primer KOR1L containing the 1/2 attB2 recombination site and the stop codon of the *KOR1* gene (5′-AAGAAAGCTGGGTCAGGTTTCCATGGTGCTGGTGGAGGTGGTGG-3′). The final construct was verified by sequencing.

Isolation of the GFP-KOR1 Seedlings, Genetic Analyses, and Molecular Complementation

kor1-1 and wild-type seedlings were transformed by infiltration using *Agrobacterium tumefaciens* carrying the GFP-KOR1 construct (Bechtold et al., 1993). T2 lines were analyzed: three lines in the wild-type background and two lines in the *kor1-1* background segregated hygromycin (25 mg/L) with a 3:1 ratio. The wild-type background lines were amplified, and homozygous lines were used in these experiments.

Hypocotyl Length Measurements

Seedlings ($n = 50$) were spread out on agar plates, and the lengths of roots and hypocotyls were measured using image-analysis software (Optimas 5; Bioscan).

Protein Extraction and Immunoblotting

Crude extracts were prepared from *Arabidopsis* seedlings. Fifty seedlings were ground in 100 μL of extraction buffer (1 M Tris-HCl, pH 7.8, 1 mM EDTA, 1 mM DTT, and 1.5 mM phenylmethylsulfonyl fluoride) and centrifuged at 13,000*g* for 10 min to remove debris. Protein gel blot analysis was performed as described by Nicol et al. (1998) with a 1:260 dilution of αNKOR1. The secondary antibody used was an anti-rabbit peroxide antibody with a 1:700 dilution (Sigma-Aldrich).

Whole-Mount Immunolocalization

The 3- to 6-d-old *Arabidopsis* seedlings were fixed in 4% paraformaldehyde in MSTB (50 mM PIPES, 5 mM EGTA, and 0.2% Triton X-100) for 1 h. Samples were washed with MSTB (two times, 15 min). Cell walls were digested with 0.2% Pectolyase, 0.8% Macerozyme, 0.4 M mannitol, and protease inhibitor for 30 min at room temperature. Samples were washed with 0.5% Triton X-100/MSTB (once for 15 min, once for 10 min) and with PBS (two times, 15 min). Seedlings were preincubated in 3% BSA/PBS for 1 h and incubated with the primary antibody (αNKOR1 diluted 1:260; c-myc diluted 1:800 [Sigma-Aldrich]) in 3% BSA/PBS overnight at 4°C. After extensive washing with PBS at room temperature (three times, 20 min), the seedlings were incubated with a secondary antibody coupled to fluorochromes (Alexa 488 and Alexa 568 diluted 1:500 [Molecular Probes]) in 3% BSA/PBS for another 2 h at 37°C. Finally, the seedlings were washed with PBS (three times, 20 min) at room temperature in the dark.

Laser Scanning Confocal Microscopy

Images were collected with a spectral Leica SP2 AOBS confocal microscope (Leica Microsystems) equipped with an argon laser and a HeNe laser. Different fluorochromes were detected using laser lines 488 nm (Alexa 488, GFP, and FM4-64) and 543 nm (Alexa 568). The images were coded green (fluorescein isothiocyanate, GFP) and red (Alexa 568, FM4-64), giving yellow colocalization in merged images. The oil objectives used were ×40 (numerical aperture 1.25), giving a resolution of 160 nm in the *x-y* plane and 330 nm along the *z* axis (pinhole 1 Airy unit). Each image shown represents either a single focal plan or a projection of individual images taken as a Z series. To determine the specificity of the signals, sequential scans were performed.

Time-lapse imaging was performed at a 512-scan format, collecting images at 10-s intervals for 4 min at a medium scan speed (450 lines/s). Twenty-five stacks of six sections were collected and assembled to process the movie. Orthogonal projections were done with Leica software (see supplemental data online).

Manual tracking was performed to measure the average velocities of GFP-KOR1–containing compartments showing linear trajectories using the Image J software (http://rsb.info.nih.gov/ij/) manual tracking plug-in developed by F. Cordelières (Institut Curie). Ten individual tracks were measured.

Quantification of Distribution and Surface of GFP-KOR1 Compartments in Root Cells

GFP-KOR1 seedlings were grown on *Arabidopsis* medium without sucrose for 3 d under light conditions. Isoxaben (4×10^{-9} M) was administered to seedlings for 1 h. Confocal microscopy observations were acquired and analyzed with Image J software. Dot surfaces were measured for every dot within the cells treated with isoxaben or DMSO (control). Concerning the analysis of the distribution of dots, the ratio was determined between the number of dots found on the upper side of the cell and the total number of dots. The upper side was defined as the volume found between the surface of the cell and the tonoplast. Each optical section analyzed was 0.5 μm deep. Student's *t* tests were

performed: *t* values for the comparison between DMSO- and 4×10^{-9} M isoxaben–treated seedlings were −6.02 and 28.14 for GFP-KOR1 compartment position and surface, respectively.

Determination of the Percentage of Colocalization between FM4-64–Labeled Structures and GFP-KOR1 Compartments in Root Cells

Colocalization was evaluated in epidermal cells of two different stages of development: small cells that started to elongate (~10 μm) and larger cells (between 50 and 70 μm). Using an adequate resolution in the *x-y* plane, 60 single optical sections from 60 individual cells were collected. In each channel, the center of each compartment was determined using a manual method. After merging images, compartments were considered colabeled if the distance between the two compartments was equal or less than the resolution (0156 μm in the *x-y* axis). The percentage of colocalization was defined as the ratio between the number of colabeled compartments and the total number of colabeled compartments and GFP-KOR1 compartments. A Student's *t* test was performed: the *t* value for the comparison between the two categories of cells was 3.78×10^{-9}.

Supplemental Data

The following materials are available in the online version of this article.

Supplemental Video 1. Orthogonal Projection from Living Root Cells Expressing the GFP-KOR1 Fusion Protein.

Supplemental Video 2. Orthogonal Projection from Living Root Cells Expressing the GFP-KOR1 Fusion Protein Treated with 4×10^{-9} M Isoxaben for 1 h.

Supplemental Video 3. Time-Lapse Movie of GFP-KOR1–Labeled Structures in a Transgenic *Arabidopsis* Root for 4 min.

ACKNOWLEDGMENTS

We thank M. Molhoj for providing the antibody against the C terminus of KOR1, C. Hawes for providing the JIM84 antibody, and P. Dupree, N. Chua, and G. Jürgens for providing Arabidopsis lines. Special thanks are given to Vera Wagner for initial help with confocal laser scanning microscopy and immunolocalization and to Suzanne Bolte and Nadine Paris for stimulating discussions. We thank G. Mouille for help with statistics. This work was funded by a grant from the Association pour la Recherche chez les Nicotianées/Institut National de la Recherche Agronomique to S.R., a grant from Amadeus Austria–France to M.-T.H. and H.H., grants from the French Ministry of Research and Technology, Action Concertée Incitative, Développement et Physiologie Intégrative (Grants 47 [2000] and 032509 [2003]) to H.H., and a grant from European Economic Community FP5 project GEMINI.

Received July 18, 2005; revised September 14, 2005; accepted October 13, 2005; published November 11, 2005.

REFERENCES

Ambrose, J.C., Li, W., Marcus, A., Ma, H., and Cyr, R. (2005). A minus-end-directed kinesin with plus-end tracking protein activity is involved in spindle morphogenesis. Mol. Biol. Cell **16,** 1584–1592.

Baskin, T.I. (2001). On the alignment of cellulose microfibrils by cortical microtubules: A review and a model. Protoplasma **215,** 150–171.

Bechtold, N., Ellis, J., and Pelletier, G. (1993). *In planta* Agrobacterium-mediated gene transfer by infiltration of adult *Arabidopsis thaliana* plants. C. R. Acad. Sci. Ser. III Sci. Vie **316,** 1194–1199.

Boevink, P., Oparka, K., Santa Cruz, S., Martin, B., Betteridge, A., and Hawes, C. (1998). Stacks on tracks: The plant Golgi apparatus traffics on an actin/ER network. Plant J. **15,** 441–447.

Bolte, S., Talbot, C., Boutte, Y., Catrice, O., Reads, N.D., and Satiat-Jeunemaître, B. (2004). FM-dyes as experimental probes for dissecting vesicle trafficking in living plant cells. J. Microsc. **214,** 159–173.

Brummell, D.A., Catala, C., Lashbrook, C.C., and Bennett, A.B. (1997). A membrane-anchored E-type endo-1,4-beta-glucanase is localized on Golgi and plasma membranes of higher plants. Proc. Natl. Acad. Sci. USA **94,** 4794–4799.

Bryant, N.J., Govers, R., and James, D.E. (2002). Regulated transport of the glucose transporter GLUT4. Nat. Rev. Mol. Cell Biol. **3,** 267–277.

Burk, D.H., and Ye, Z.H. (2002). Alteration of oriented deposition of cellulose microfibrils by mutation of a katanin-like microtubule-severing protein. Plant Cell **14,** 2145–2160.

Cutler, S.R., Ehrhardt, D.W., Griffitts, J.S., and Somerville, C.R. (2000). Random GFP::cDNA fusions enable visualization of subcellular structures in cells of Arabidopsis at a high frequency. Proc. Natl. Acad. Sci. USA **97,** 3718–3723.

Desprez, T., Vernhettes, S., Fagard, M., Refregier, G., Desnos, T., Aletti, E., Py, N., Pelletier, S., and Hofte, H. (2002). Resistance against herbicide isoxaben and cellulose deficiency caused by distinct mutations in same cellulose synthase isoform CESA6. Plant Physiol. **128,** 482–490.

Doblin, M.S., Kurek, I., Jacob-Wilk, D., and Delmer, D.P. (2002). Cellulose biosynthesis in plants: From genes to rosettes. Plant Cell Physiol. **43,** 1407–1420.

Dunkley, T.P., Watson, R., Griffin, J.L., Dupree, P., and Lilley, K.S. (2004). Localization of organelle proteins by isotope tagging (LOPIT). Mol. Cell. Proteomics **3,** 1128–1134.

Ellis, C., Karafyllidis, I., Wasternack, C., and Turner, J.G. (2002). The Arabidopsis mutant *cev1* links cell wall signaling to jasmonate and ethylene responses. Plant Cell **14,** 1557–1566.

Estelle, M.A., and Somerville, C.R. (1987). Auxin-resistant mutants of *Arabidopsis thaliana* with an altered morphology. Mol. Gen. Genet. **206,** 200–206.

Fagard, M., Desnos, T., Desprez, T., Goubet, F., Refregier, G., Mouille, G., McCann, M., Rayon, C., Vernhettes, S., and Hofte, H. (2000). *PROCUSTE1* encodes a cellulose synthase required for normal cell elongation specifically in roots and dark-grown hypocotyls of Arabidopsis. Plant Cell **12,** 2409–2424.

Gardiner, J.C., Taylor, N.G., and Turner, S.R. (2003). Control of cellulose synthase complex localization in developing xylem. Plant Cell **15,** 1740–1748.

Geldner, N., Anders, N., Wolters, H., Keicher, J., Kornberger, W., Muller, P., Delbarre, A., Ueda, T., Nakano, A., and Jurgens, G. (2003). The Arabidopsis GNOM ARF-GEF mediates endosomal recycling, auxin transport, and auxin-dependent plant growth. Cell **112,** 219–230.

Geldner, N., Friml, J., Stierhof, Y.-D., Jurgens, G., and Palme, K. (2001). Auxin transport inhibitors block PIN1 cycling and vesicle trafficking. Nature **413,** 425–428.

Grebe, M., Xu, J., Mobius, W., Ueda, T., Nakano, A., Geuze, H.J., Rook, M.B., and Scheres, B. (2003). Arabidopsis sterol endocytosis involves actin-mediated trafficking *via* ARA6-positive early endosomes. Curr. Biol. **13,** 1378–1387.

Hawes, C., and Satiat-Jeunemaitre, B. (2005). The plant Golgi apparatus—Going with the flow. Biochim. Biophys. Acta **1744,** 466–480.

Himmelspach, R., Williamson, R.E., and Wasteneys, G.O. (2003). Cellulose microfibril alignment recovers from DCB-induced disruption despite microtubule disorganization. Plant J. **36,** 565–575.

His, I., Driouich, A., Nicol, F., Jauneau, A., and Höfte, H. (2001). Altered pectin composition in primary cell walls of korrigan, a dwarf mutant of Arabidopsis deficient in a membrane-bound endo-1,4 beta-glucanase. Planta **212,** 348–358.

Lane, D.R., et al. (2001). Temperature-sensitive alleles of RSW2 link the KORRIGAN endo-1,4-beta-glucanase to cellulose synthesis and cytokinesis in Arabidopsis. Plant Physiol. **126,** 278–288.

Marcus, A.I., Ambrose, J.C., Blickley, L., Hancock, W.O., and Cyr, R.J. (2002). *Arabidopsis thaliana* protein, ATK1, is a minus-end directed kinesin that exhibits non-processive movement. Cell Motil. Cytoskeleton **52,** 144–150.

Master, E.R., Rudsander, U.J., Zhou, W., Henriksson, H., Divne, C., Denman, S., Wilson, D.B., and Teeri, T.T. (2004). Recombinant expression and enzymatic characterization of PttCel9A, a KOR homologue from *Populus tremula* × *tremuloides.* Biochemistry **43,** 10080–10089.

Melan, M.A. (1990). Taxol maintains organized microtubule patterns in protoplasts which lead to the resynthesis of organized cell wall microfibrils. Protoplasma **153,** 169–177.

Mikyoung, P., Penick, C.E., Edwards, J.G., Kauer, J.A., and Ehlers, M.D. (2004). Recycling endosomes supply AMPA receptors for LTP. Science **305,** 1972–1975.

Molhoj, M., Pagant, S., and Hofte, H. (2002). Towards understanding the role of membrane-bound endo-beta-1,4-glucanases in cellulose biosynthesis. Plant Cell Physiol. **43,** 1399–1406.

Molhoj, M., Ulvskov, P., and Dal Degan, F. (2001). Characterization of a functional soluble form of a *Brassica napus* membrane-anchored endo-1,4-beta-glucanase heterologously expressed in *Pichia pastoris.* Plant Physiol. **127,** 674–684.

Mulder, B., Schel, J., and Emons, A.M. (2004). How the geometrical model for plant cell wall formation enables production of a random texture. Cellulose **11,** 395–401.

Nebenfuhr, A., Gallagher, L.A., Dunahay, T.G., Frohlick, J.A., Mazurkiewicz, A.M., Meehl, J.B., and Staehelin, L.A. (1999). Stop-and-go movements of plant Golgi stacks are mediated by the acto-myosin system. Plant Physiol. **121,** 1127–1142.

Nicol, F., His, I., Jauneau, A., Vernhettes, S., Canut, H., and Hofte, H. (1998). A plasma membrane-bound putative endo-1,4-beta-D-glucanase is required for normal wall assembly and cell elongation in Arabidopsis. EMBO J. **17,** 5563–5576.

Paciorek, T., Zazimalova, E., Ruthardt, N., Petrasek, J., Stierhof, Y.D., Klein-Vehn, J., Morris, D.A., Emans, N., Jürgens, G., Geldner, N., and Friml, J. (2005). Auxin inhibits endocytosis and promotes its own efflux from cells. Nature **435,** 1254–1256.

Peng, L., Kawagoe, Y., Hogan, P., and Delmer, D. (2002). Sitosterol-beta-glucoside as primer for cellulose synthesis in plants. Science **295,** 147–150.

Roberg, K.J., Rowley, N., and Kaiser, C.A. (1997). Physiological regulation of membrane protein sorting late in the secretory pathway of *Saccharomyces cerevisiae.* J. Cell Biol. **137,** 1469–1482.

Robert, S., Mouille, G., and Höfte, H. (2004). The mechanism and regulation of cellulose synthesis in primary walls: Lessons from cellulose deficient Arabidopsis mutants. Cellulose **11,** 351–364.

Roudier, F., Fernandez, A.G., Fujita, M., Himmelspach, R., Borner, G.H., Schindelman, G., Song, S., Baskin, T.I., Dupree, P., Wasteneys, G.O., and Benfey, P.N. (2005). COBRA, an Arabidopsis extracellular glycosyl-phosphatidyl inositol-anchored protein, specifically controls highly anisotropic expansion through its involvement in cellulose microfibril orientation. Plant Cell **17,** 1749–1763.

Satiat-Jeunemaitre, B., and Hawes, C. (1992). Redistribution of a Golgi glycoprotein in plant cells treated with brefeldin A. J. Cell Sci. **103,** 1153–1166.

Satiat-Jeunemaitre, B., and Hawes, C. (1994). G.A.T.T. (A General Agreement on Traffic and Transport) and brefeldin A in plant cells. Plant Cell **6,** 463–467.

Sato, S., Kato, T., Kakegawa, K., Ishii, T., Liu, Y.G., Awano, T., Takabe, K., Nishiyama, Y., Kuga, S., Nakamura, Y., Tabata, S., and Shibata, D. (2001). Role of the putative membrane-bound endo-1,4-beta-glucanase KORRIGAN in cell elongation and cellulose synthesis in *Arabidopsis thaliana.* Plant Cell Physiol. **42,** 251–263.

Scheible, W.R., Eshed, R., Richmond, T., Delmer, D., and Somerville, C. (2001). Modifications of cellulose synthase confer resistance to isoxaben and thiazolidinone herbicides in Arabidopsis *Ixr1* mutants. Proc. Natl. Acad. Sci. USA **98,** 10079–10084.

Schrick, K., Fujioka, S., Takatsuto, S., Stierhof, Y.D., Stransky, H., Yoshida, S., and Jurgens, G. (2004). A link between sterol biosynthesis, the cell wall, and cellulose in Arabidopsis. Plant J. **38,** 227–243.

Szyjanowicz, P.M., McKinnon, I., Taylor, N.G., Gardiner, J., Jarvis, M.C., and Turner, S.R. (2004). The irregular xylem 2 mutant is an allele of korrigan that affects the secondary cell wall of *Arabidopsis thaliana.* Plant J. **37,** 730–740.

Taylor, N.G., Howells, R.M., Huttly, A.K., Vickers, K., and Turner, S.R. (2003). Interactions among three distinct CesA proteins essential for cellulose synthesis. Proc. Natl. Acad. Sci. USA **100,** 1450–1455.

Taylor, N.G., Laurie, S., and Turner, S.R. (2000). Multiple cellulose synthase catalytic subunits are required for cellulose synthesis in Arabidopsis. Plant Cell **12,** 2529–2540.

Taylor, N.G., Scheible, W.R., Cutler, S., Somerville, C.R., and Turner, S.R. (1999). The *irregular xylem3* locus of Arabidopsis encodes a cellulose synthase required for secondary cell wall synthesis. Plant Cell **11,** 769–780.

Tominaga, M., Kojima, H., Yokota, E., Orii, H., Nakamori, R., Katayama, E., Anson, M., Shimmen, T., and Oiwa, K. (2003). Higher plant myosin XI moves processively on actin with 35 nm steps at high velocity. EMBO J. **22,** 1263–1272.

Ueda, T., Yamaguchi, M., Uchimiya, H., and Nakano, A. (2001). Ara6, a plant-unique novel type Rab GTPase, functions in the endocytic pathway of *Arabidopsis thaliana.* EMBO J. **20,** 4730–4741.

Valdivia, R.H., and Schekman, R. (2003). The yeasts Rho1p and Pkc1p regulate the transport of chitin synthase III (Chs3p) from internal stores to the plasma membrane. Proc. Natl. Acad. Sci. USA **100,** 10287–10292.

Vida, T.A., and Emr, S.D. (1995). A new vital stain for visualizing vacuolar membrane dynamics and endocytosis in yeast. J. Cell Biol. **128,** 779–792.

Wasteneys, G.O. (2004). Progress in understanding the role of microtubules in plant cells. Curr. Opin. Plant Biol. **7,** 651–660.

Zuo, J., Niu, Q.W., Nishizawa, N., Wu, Y., Kost, B., and Chua, N.H. (2000). KORRIGAN, an Arabidopsis endo-1,4-beta-glucanase, localizes to the cell plate by polarized targeting and is essential for cytokinesis. Plant Cell **12,** 1137–1152.